Homework 3 in EL2450 Hybrid and Embedded Control Systems

First name1 Last name1
person number
email

First name2 Last name2
person number
email

First name3 Last name3
person number
email

First name4 Last name4
person number
email

Task 1

$$\begin{aligned} u_\omega &= \frac{u_r + u_l}{2} \\ u_\Psi &= u_r - u_l \end{aligned} \quad \Leftrightarrow \quad \begin{aligned} u_l &= u_\omega - \frac{u_\Psi}{2} \\ u_r &= u_\omega + \frac{u_\Psi}{2} \end{aligned}$$

Task 2

Task 3

In order to reach a conclusion about the stability of the angular displacement, it suffices to find a Lyapunov function $V(x)$ such that $V(0) = 0$, $V(x) > 0$ for all $x \neq 0$ and $\dot{V}(x) \leq 0$ for all x. Considering $x = \theta - \theta^G$ and $V(x) = x^2$:

$$V(0) = 0,\ V(x) > 0,\ \text{for all } x \neq 0, \text{ and}$$

$$\begin{aligned} \dot{V}(x) &= 2x\dot{x} = 2(\theta - \theta^G)\dot{\theta} \\ &= 2(\theta - \theta^G)\frac{R}{L}u_\Psi \end{aligned}$$

- When $\theta - \theta^G \leq 0$, $\dot{V}(x) = 2(\theta - \theta^G)\frac{R}{L} \leq 0$
- When $\theta - \theta^G > 0$, $\dot{V}(x) = -2(\theta - \theta^G)\frac{R}{L} < 0$

Hence $\dot{V}(x) \leq 0$ for all x, meaning that the system is stable for all $\theta \in (-180°, 180°]$.

Task 4

Examining file `rot2.slx` one sees that $\dot{\theta} = R/Lu_\Psi$ is stable. We can verify this analytically:

$$\begin{aligned}
\dot{u}_\Psi &= K_L(u_\Psi^R - u_\Psi) \\
\dot{u}_\Psi &= K_L u_\Psi^R - K_L u_\Psi \\
\dot{u}_\Psi \cdot e^{K_L t} &= K_L u_\Psi^R \cdot e^{K_L t} - K_L u_\Psi \cdot e^{K_L t} \\
\dot{u}_\Psi \cdot e^{K_L t} + K_L u_\Psi \cdot e^{K_L t} &= K_L u_\Psi^R \cdot e^{K_L t} \\
\frac{d}{dt}(u_\Psi e^{K_L t}) &= K_L u_\Psi^R e^{K_L t} \\
u_\Psi e^{K_L t} &= \int K_L u_\Psi^R e^{K_L t} = u_\Psi^R e^{K_L t} + \lambda \\
u_\Psi &= u_\Psi^R + \lambda e^{-K_L t}
\end{aligned}$$

Where, from inspection of the parameters of the integrator, the initial condition is $\lambda = 1$. Hence

$$u_\Psi(t) = \begin{cases} 1 + e^{-K_L t} & \theta - \theta^G \leq 0 \\ -1 + e^{-K_L t} & \theta - \theta^G > 0 \end{cases} \tag{1}$$

In order to reach a conclusion about the stability of the angular displacement, it suffices to find a Lyapunov function $V(x)$ such that $V(0) = 0$, $V(x) > 0$ for all $x \neq 0$ and $\dot{V}(x) \leq 0$ for all x. Considering $x = \theta - \theta^G$ and $V(x) = x^2$:

$$V(0) = 0,\ V(x) > 0,\ \text{for all } x \neq 0, \text{ and}$$

$$\begin{aligned}
\dot{V}(x) = 2x\dot{x} &= 2(\theta - \theta^G)\dot{\theta} \\
&= 2(\theta - \theta^G)\frac{R}{L}u_\Psi \\
&= 2(\theta - \theta^G)\frac{R}{L}(u_\Psi^R + e^{-K_L t})
\end{aligned}$$

- When $\theta - \theta^G \leq 0$, $\dot{V}(x) = 2(\theta - \theta^G)\frac{R}{L}(1 + e^{-K_L t}) \leq 0$
  With

$$\begin{aligned}
0 < e^{-K_L t} &\leq 1 \\
0 < 1 < 1 + e^{-K_L t} &\leq 2
\end{aligned} \tag{2}$$

- When $\theta - \theta^G > 0$, $\dot{V}(x) = 2(\theta - \theta^G)\frac{R}{L}(-1 + e^{-K_L t}) < 0$
  With

$$\begin{aligned}
0 < e^{-K_L t} &\leq 1 \\
-1 < -1 + e^{-K_L t} &\leq 0
\end{aligned} \tag{3}$$

Hence, from inequalities 2 and 3 we conclude that $\dot{V}(x) \leq 0$ for all x, meaning that the system is stable for all $\theta \in (-180°, 180°]$.

Task 5

Task 6

Task 7

$$\begin{aligned}\theta[k+1] &= \theta[k] + \frac{T_s R}{L} u_\Psi^R[k] \\ &= \theta[k] + \frac{T_s R}{L} K_\Psi^R(\theta^R - \theta[k]) \\ &= \theta[k](1 - \frac{T_s R}{L} K_\Psi^R) + \frac{T_s R}{L} K_\Psi^R \theta^R\end{aligned}$$

By subtracting θ^R from both sides one gets

$$\begin{aligned}\theta[k+1] - \theta^R &= \theta[k](1 - \frac{T_s R}{L} K_\Psi^R) + (\frac{T_s R}{L} K_\Psi^R - 1)\theta^R \\ &= (\theta[k] - \theta^R)(1 - \frac{T_s R}{L} K_\Psi^R) \qquad (4)\end{aligned}$$

We now define state θ' as

$$\theta'[k] = \theta[k] - \theta^R$$

Then, equation 4 becomes

$$\theta'[k+1] = \theta'[k](1 - \frac{T_s R}{L} K_\Psi^R)$$

In order for this system to be stable, that is, $|\theta - \theta^R| \to 0$ as $k \to \infty$, the solution of the equation inside the parentheses should lie inside the unit circle:

$$\begin{aligned}\left|1 - \frac{T_s R}{L} K_\Psi^R\right| &< 1 \\ -1 < 1 - \frac{T_s R}{L} K_\Psi^R &< 1 \\ -2 < -\frac{T_s R}{L} K_\Psi^R &< 0 \\ 0 < \frac{T_s R}{L} K_\Psi^R &< 2 \\ 0 < K_\Psi^R &< \frac{2L}{T_s R} \qquad (5)\end{aligned}$$

Hence, the maximum value K_Ψ^R can take for the system to be marginally stable is $K_{\Psi,max}^R = \frac{2L}{T_s R}$

Theoretically, the value of K_Ψ^R can be chosen to be any value inside the interval defined in inequality 5. However, first, it would be wise to choose a value that is far enough from the maximum value so as to avoid overshoot, but close enough to it, so that convergence happens in reasonable time. Hence, in practice, it is reasonable that one would need to experiment with different values and choose one that results in balancing a small angular error, a minimal overshoot, if any, and a quick enough settling time.

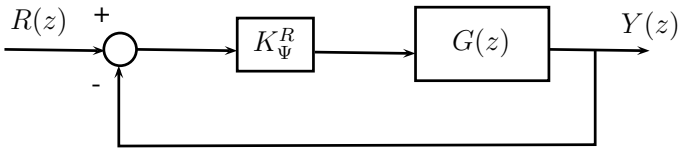

Figure 1: The structure of the system under rotational control. $G(z)$ is the discretized transfer function of the linear system whose state-space equation is $\dot{\theta} = \frac{R}{L} u_\Psi$

Task 8

For the purpose of simulating this part of the controller, the initial point of the robot was taken to be $I(x_0, y_0) \equiv (0, 0)$. The goal was set to $G(x_g, y_g) \equiv (-0.37, 1.68)$, which is node 1 in the simulation environment. The angle between the line connecting I and G and the x-axis is hence $\theta_R = tan^{-1}(1.68/-0.37) = 102.42$ degrees.

Figures 2, 4, 6, 8, 10 show the angular response of the robot for different values of K_Ψ^R inside the interval set by inequality 5. Figure 12 verifies that the upper limit for K_Ψ^R is indeed $K_{\Psi,max}^R = \frac{2L}{T_s R}$ by showing that the angular response of the robot cannot converge for $K_\Psi^R > K_{\Psi,max}^R$.

Here, one can see that the smaller the value of K_Ψ^R is, the larger the settling time, the lower the rise time and the smoother the response is. However, as the value of K_Ψ^R increases, the steady-state response begins to oscillate, with the amplitude of this oscillation proportional to the value of K_Ψ^R.

Figures 3, 5, 7, 9 and 3 focus on the steady-state value of the aforementioned responses. As it is evident, none of the responses converge to the value $\theta_R = 102.42$. This is reasonable since with only a purely proportional control signal, as the angular error, i.e. $e(\theta) = \theta^R - \theta$, tends to zero, the product of K_Ψ^R and $e(\theta)$ isn't large enough to force the robot to rotate exactly θ^R degrees.

Another way to look at this is by looking at the steady-state response of the system, which is linear, for a step input of magnitude θ^R. Figure 1 shows the structure of the system. The z-transform of the input is then $R(z) = \dfrac{\theta^R}{1 - z^{-1}}$ and the equation of the closed-loop system is

$$Y(z) = \frac{K_\Psi^R G(z)}{1 + K_\Psi^R G(z)} R(z)$$

The steady-state response is

$$lim_{t\to\infty} y(t) = lim_{z\to 1}(1 - z^{-1}) \frac{\theta^R}{1 - z^{-1}} \frac{K_\Psi^R G(z)}{1 + K_\Psi^R G(z)} = \theta^R \cdot lim_{z\to 1} \frac{K_\Psi^R G(z)}{1 + K_\Psi^R G(z)}$$

The steady-state response cannot reach exactly θ^R as the above limit cannot converge to 1 under our limitations for K_Ψ^R and the dynamics of $G(z)$.

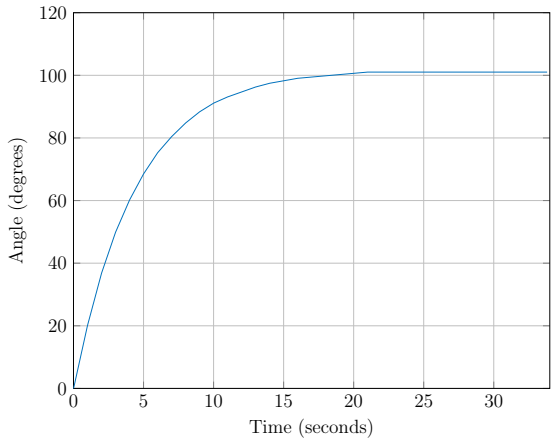

Figure 2: The orientation of the robot over time for $K_{\Psi}^{R} = 0.1K_{\Psi,max}^{R}$

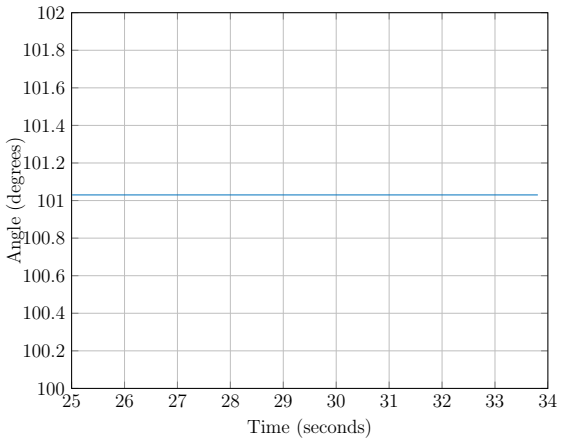

Figure 3: The steady state orientation of the robot for $K_{\Psi}^{R} = 0.1K_{\Psi,max}^{R}$

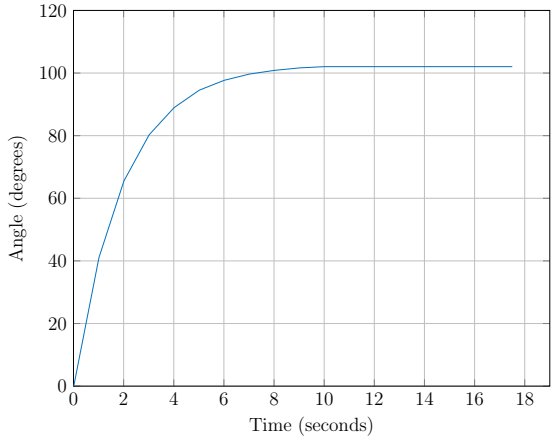

Figure 4: The orientation of the robot over time for $K_{\Psi}^{R} = 0.2K_{\Psi,max}^{R}$

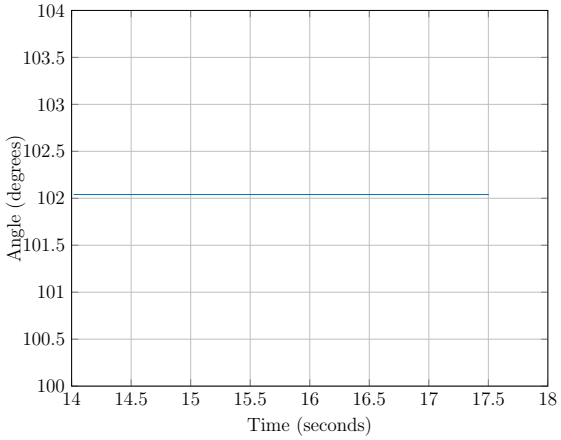

Figure 5: The steady state orientation of the robot for $K_{\Psi}^{R} = 0.2K_{\Psi,max}^{R}$

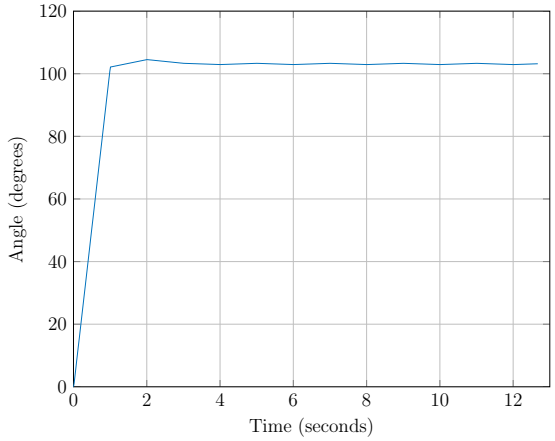

Figure 6: The orientation of the robot over time for $K_{\Psi}^{R} = 0.5K_{\Psi,max}^{R}$

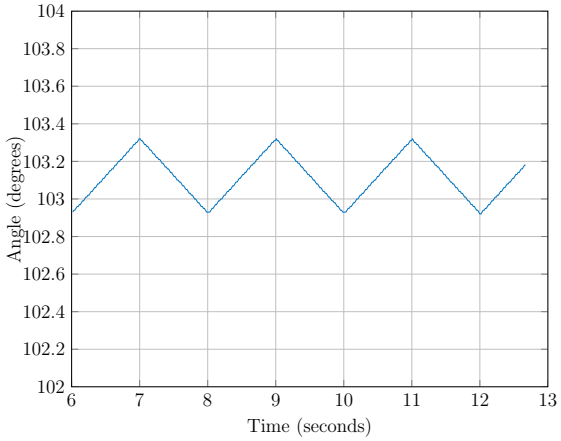

Figure 7: The steady state orientation of the robot for $K_{\Psi}^{R} = 0.5K_{\Psi,max}^{R}$

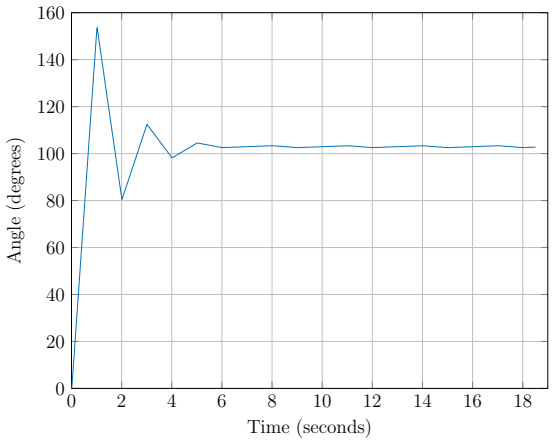

Figure 8: The orientation of the robot over time for $K_{\Psi}^{R} = 0.75K_{\Psi,max}^{R}$

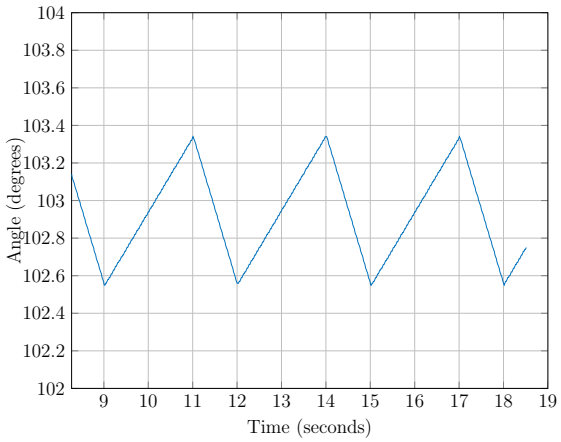

Figure 9: The steady state orientation of the robot for $K_{\Psi}^{R} = 0.75K_{\Psi,max}^{R}$

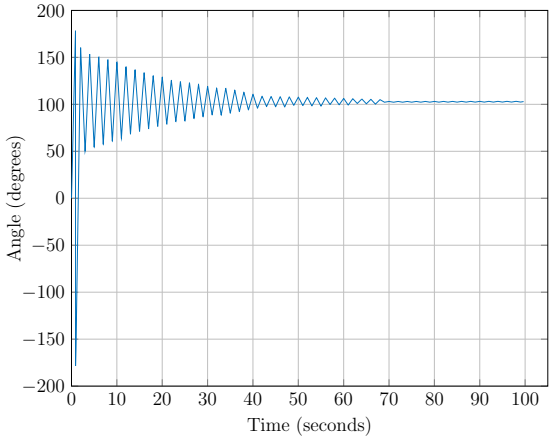

Figure 10: The orientation of the robot over time for $K_{\Psi}^{R} = K_{\Psi,max}^{R}$. This is the upper limit value of K_{Ψ}^{R} before the system becomes unstable

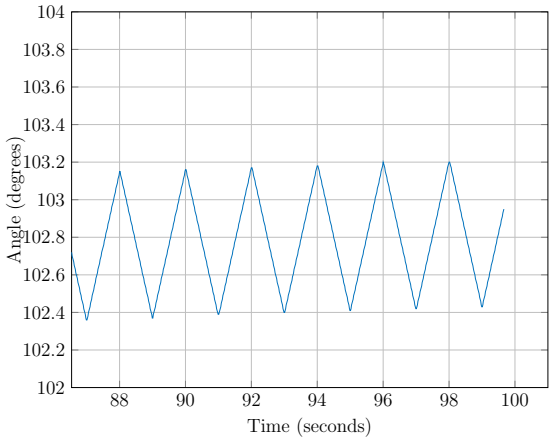

Figure 11: The steady state orientation of the robot for $K_{\Psi}^{R} = K_{\Psi,max}^{R}$

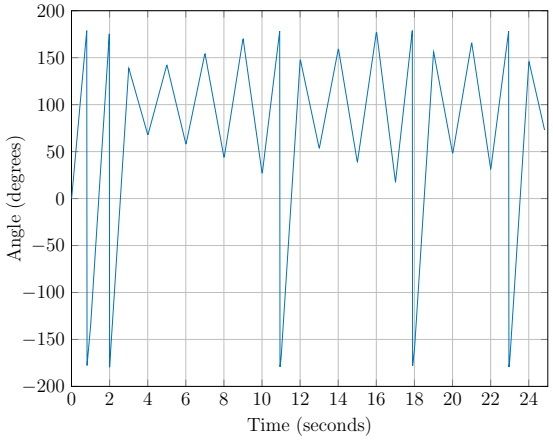

Figure 12: The orientation of the robot over time for $K_\Psi^R = K_{\Psi,max}^R + 1$. The system is indeed unstable

Task 9

$$
\begin{aligned}
d_0[k] &= cos(\theta[k])(x_0 - x[k]) + sin(\theta[k])(y_0 - y[k]) \\
&= cos(\theta[k])(x_0 - x[k-1] - T_s R u_\omega^R[k-1] cos(\theta[k-1])) \\
&+ sin(\theta[k])(y_0 - y[k-1] - T_s R u_\omega^R[k-1] sin(\theta[k-1])) \\
&= cos(\theta^R)(x_0 - x[k-1] - T_s R u_\omega^R[k-1] cos(\theta^R)) \\
&+ sin(\theta^R)(y_0 - y[k-1] - T_s R u_\omega^R[k-1] sin(\theta^R)) \\
&= cos(\theta^R)(x_0 - x[k-1]) + sin(\theta^R)(y_0 - y[k-1]) - T_s R K_\omega^T d_0[k-1] \\
&= d_0[k-1] - T_s R K_\omega^T d_0[k-1] \\
&= (1 - T_s R K_\omega^R) d_0[k-1]
\end{aligned}
$$

Hence

$$d_0[k+1] = (1 - T_s R K_\omega^R) d_0[k]$$

In order for this system to be stable, that is, $d_0 \to 0$ as $k \to \infty$, the solution of the equation inside the parentheses should lie inside the unit circle:

$$
\begin{aligned}
\left|1 - T_s R K_\omega^R\right| &< 1 \\
-1 < 1 - T_s R K_\omega^R &< 1 \\
-2 < -T_s R K_\omega^R &< 0 \\
0 < T_s R K_\omega^R &< 2 \\
0 < K_\omega^R &< \frac{2}{T_s R}
\end{aligned} \tag{6}
$$

Hence, the maximum value K_ω^R can take for the system to be marginally stable is $K_{\omega,max}^R = \dfrac{2}{T_s R}$.

Theoretically, the value of K_ω^R can be chosen to be any value inside the interval defined in inequality 6. However, first, it would be wise to choose a value that is far enough from the maximum value so as to avoid overshoot, but close enough to it, so that convergence happens in reasonable time. Hence, in practice, it is reasonable that one would need to experiment with different values and choose one that results in balancing a small angular error, a minimal overshoot, if any, and a quick enough settling time.

Task 10

This part of the controller is responsible for compensating translational errors during rotation. Since the rotational speed u_Ψ is zero, it is expected that the robot will not move away from its origin. Figure 13 plots the robot's distance from its origin over time for $K_\omega^R = 0.5K_{\omega,max}^R$.

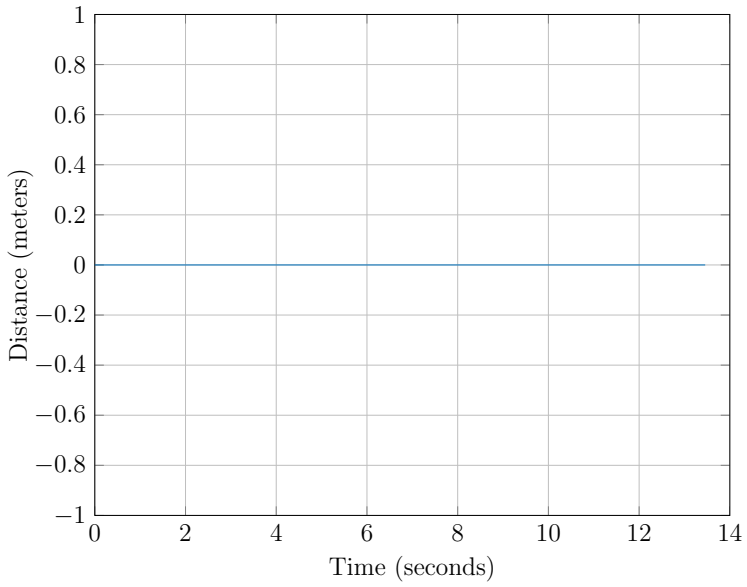

Figure 13: The distance of the robot from its origin position over time for $K_\omega^R = 0.5K_{\omega,max}^R$

Task 11

Figures 14, 16, 18, 20, 22 show the bearing error of the robot for different values of K_Ψ^R inside the interval set by inequality 5. Figures 15, 17, 19, 21 and 15 focus on the steady-state bearing error. Figure 24 illustrates the $d_0[k]$ error, which is at all times zero.

The evolution of the bearing and distance error is the same when both of the rotational controllers are enabled compared to when only one of them is enabled. This happens because the behaviour of each controller does not affect the behaviour of the other, since this is an ideal system. In reality, we expect that the distance error will be non-zero.

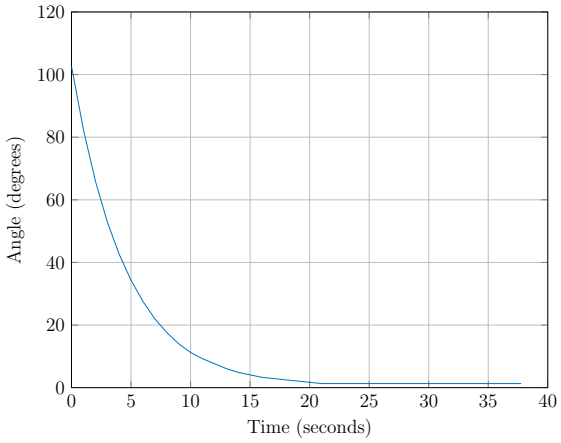

Figure 14: The error in orientation of the robot over time for $K_{\Psi}^{R} = 0.1K_{\Psi,max}^{R}$

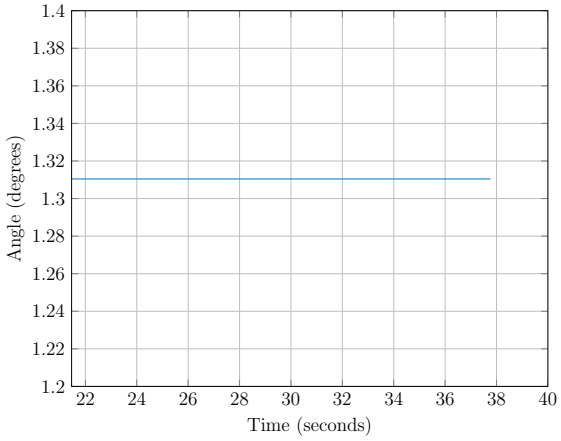

Figure 15: The steady state error in orientation of the robot for $K_{\Psi}^{R} = 0.1K_{\Psi,max}^{R}$

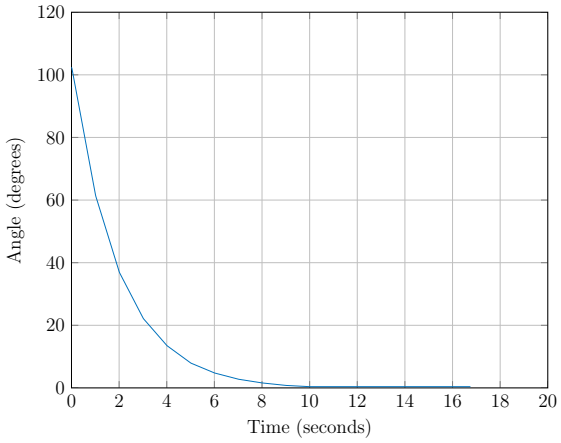

Figure 16: The error in orientation of the robot over time for $K_{\Psi}^{R} = 0.2K_{\Psi,max}^{R}$

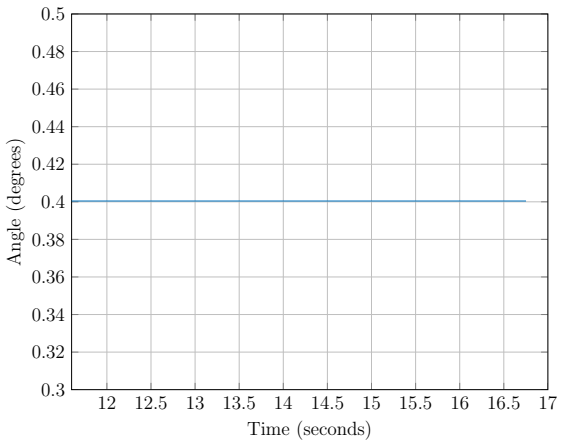

Figure 17: The steady state error in orientation of the robot for $K_{\Psi}^{R} = 0.2K_{\Psi,max}^{R}$

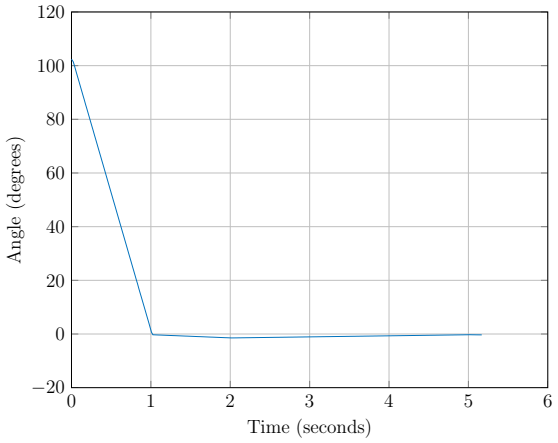

Figure 18: The error in orientation of the robot over time for $K_{\Psi}^{R} = 0.5K_{\Psi,max}^{R}$

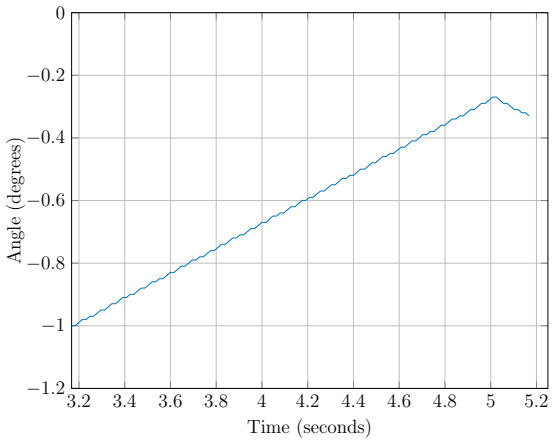

Figure 19: The steady state error in orientation of the robot for $K_{\Psi}^{R} = 0.5K_{\Psi,max}^{R}$

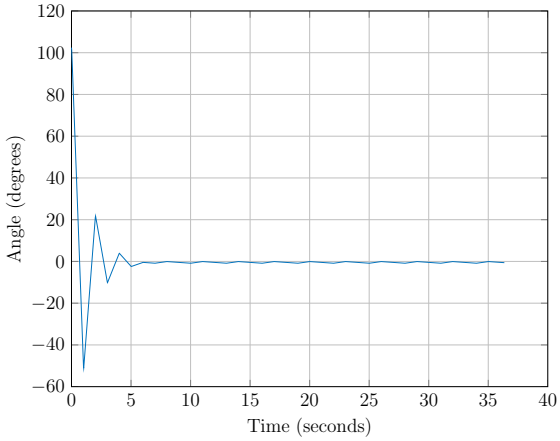

Figure 20: The error in orientation of the robot over time for $K_{\Psi}^{R} = 0.75K_{\Psi,max}^{R}$

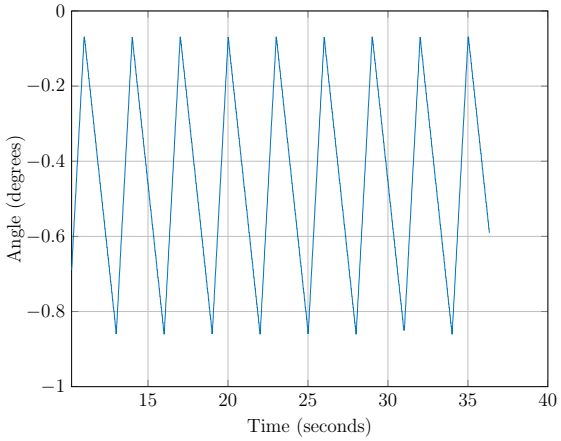

Figure 21: The steady state error in orientation of the robot for $K_{\Psi}^{R} = 0.75K_{\Psi,max}^{R}$

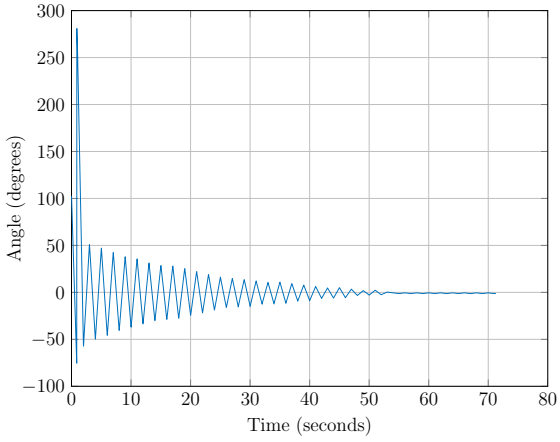

Figure 22: The error in orientation of the robot over time for $K_{\Psi}^{R} = K_{\Psi,max}^{R}$.

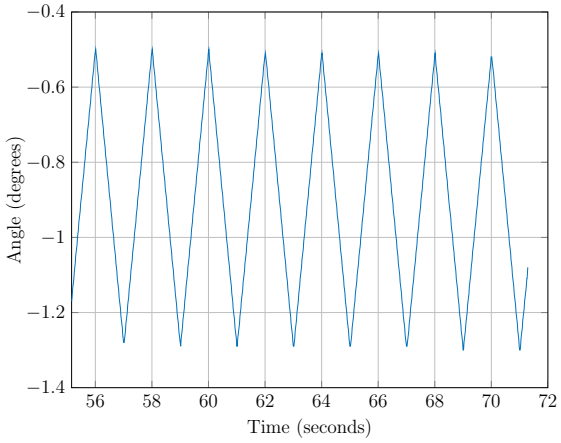

Figure 23: The steady state error in orientation of the robot for $K_{\Psi}^{R} = K_{\Psi,max}^{R}$

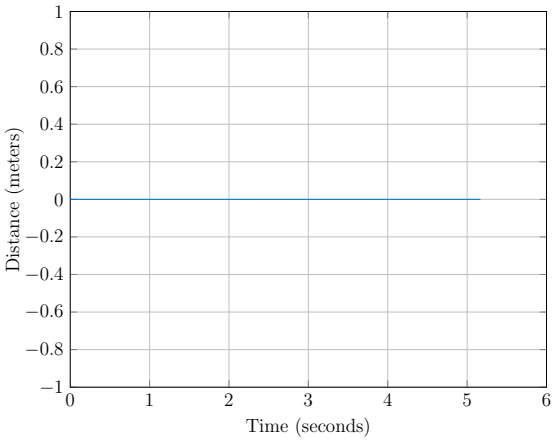

Figure 24: The distance of the robot from its origin position over time for all legitimate values or K_ω^R

Task 12

$$\begin{aligned}
d_g[k] &= cos(\theta_g)(x_g - x[k]) + sin(\theta_g)(y_g - y[k]) \\
&= cos(\theta_g)(x_g - x[k-1] - T_s R u_\omega^T[k-1] cos(\theta_g)) + \\
&sin(\theta_g)(y_g - y[k-1] - T_s R u_\omega^T[k-1] sin(\theta_g)) \\
&= cos(\theta_g)(x_g - x[k-1]) + sin(\theta_g)(y_g - y[k-1]) - T_s R K_\omega^T d_g[k-1] \\
&= d_g[k-1] - T_s R K_\omega^T d_g[k-1] \\
&= (1 - T_s R K_\omega^T) d_g[k-1]
\end{aligned}$$

Hence

$$d_g[k+1] = (1 - T_s R K_\omega^T) d_g[k]$$

In order for this system to be stable, that is, $d_g \to 0$ as $k \to \infty$, the solution of the equation inside the parentheses should lie inside the unit circle:

$$\begin{aligned}
\left|1 - T_s R K_\omega^T\right| &< 1 \\
-1 < 1 - T_s R K_\omega^T &< 1 \\
-2 < -T_s R K_\omega^T &< 0 \\
0 < T_s R K_\omega^T &< 2 \\
0 < K_\omega^T &< \frac{2}{T_s R}
\end{aligned} \tag{7}$$

Hence, the maximum value K_ω^T can take for the system to be marginally stable is $K_{\omega,max}^T = \dfrac{2}{T_s R}$

Theoretically, the value of K_ω^T can be chosen to be any value inside the interval defined in inequality 7. However, first, it would be wise to choose a value that is far enough from

the maximum value so as to avoid overshoot, but close enough to it, so that convergence happens in reasonable time. Hence, in practice, it is reasonable that one would need to experiment with different values and choose one that results in balancing a small angular error, a minimal overshoot, if any, and a quick enough settling time.

Task 13

For the purpose of simulating this part of the controller, the initial point of the robot was taken to be $I(x_0, y_0) \equiv (0, 0)$. The goal was set to $G(x_g, y_g) \equiv (1.0, 0.0)$.

Figures 25, 27, 29, 31 and 33 show the displacemental response of the robot for various values of K_ω^T inside the interval set by inequality 7. Figure 35 verifies that the upper limit for K_ω^T is indeed $\frac{2}{T_s R}$ by showing that the displacemental response of the robot cannot converge for $K_\omega^T > K_{\omega,max}^T$.

Here, one can see that the smaller the value of K_ω^T is, the larger the settling time, the lower the rise time and the smoother the response is. However, as the value of K_ω^T increases, the steady-state response begins to oscillate, with the amplitude of this oscillation proportional to the value of K_ω^T.

Figures 26, 28, 30, 32 and 34 focus on the steady-state value of the aforementioned responses. In contrast to the proportional rotational controller, the robot *can* arrive to its reference signal. The equations that govern the robot's translational movement are non-linear, as opposed to the one that governs its rotational movement, which in turn means that the translational system's behaviour is not bounded within the laws that govern control with proportional controllers on linear systems.

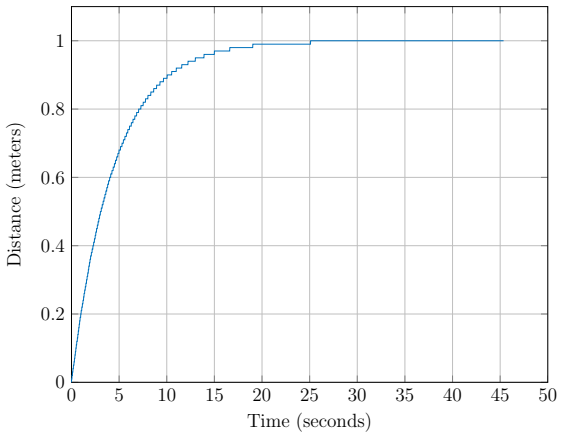

Figure 25: The orientation of the robot over time for $K_\omega^T = 0.1 K_{\omega,max}^T$

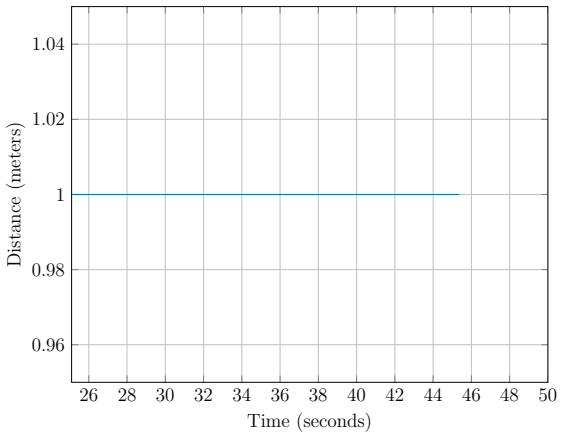

Figure 26: The steady state orientation of the robot for $K_\omega^T = 0.1 K_{\omega,max}^T$

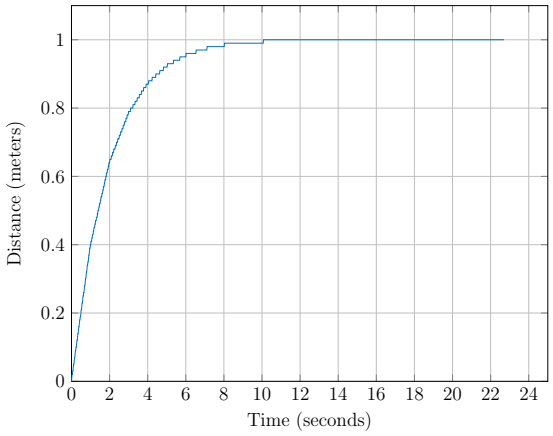

Figure 27: The orientation of the robot over time for $K_\omega^T = 0.2K_{\omega,max}^T$

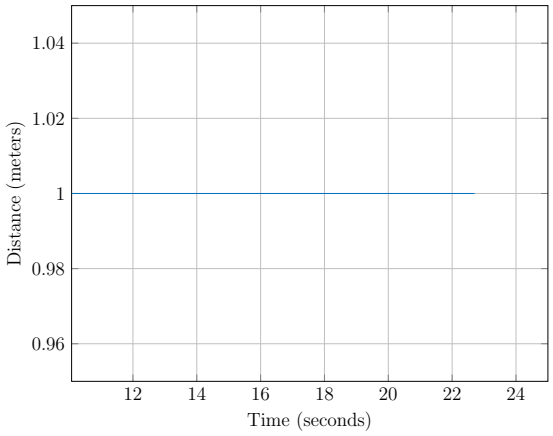

Figure 28: The steady state orientation of the robot for $K_\omega^T = 0.2K_{\omega,max}^T$

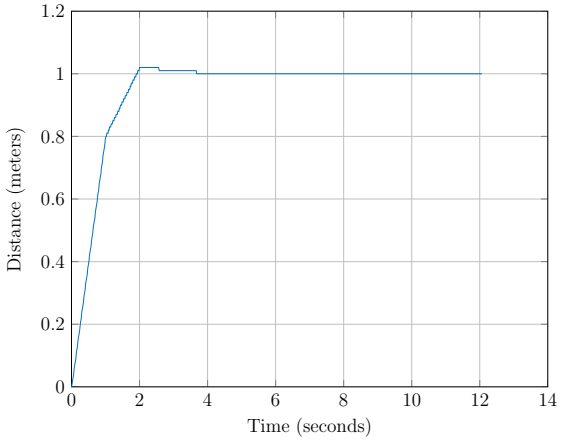

Figure 29: The orientation of the robot over time for $K_\omega^T = 0.5K_{\omega,max}^T$

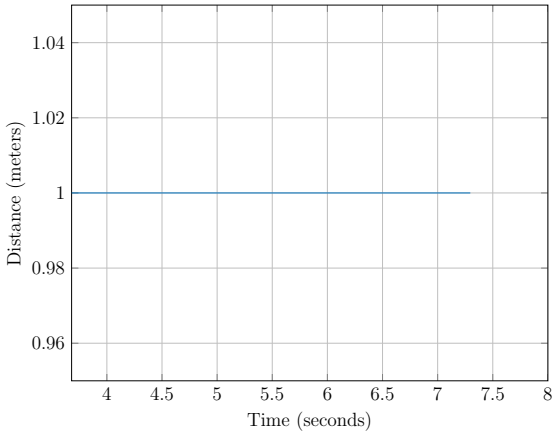

Figure 30: The steady state orientation of the robot for $K_\omega^T = 0.5K_{\omega,max}^T$

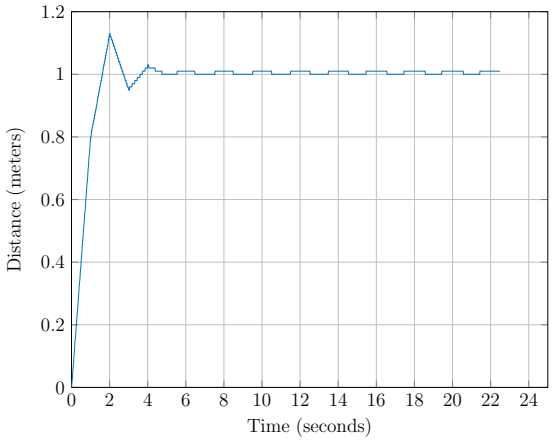

Figure 31: The orientation of the robot over time for $K_\omega^T = 0.75K_{\omega,max}^T$

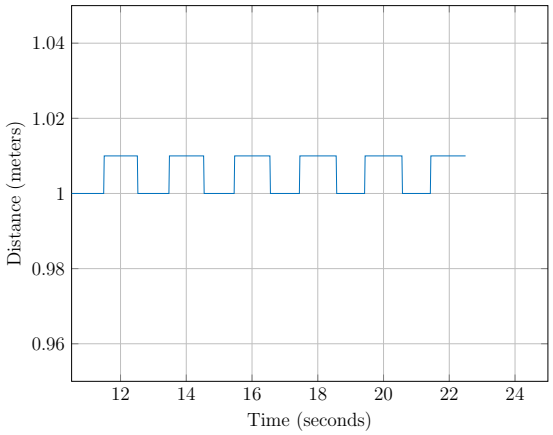

Figure 32: The steady state orientation of the robot for $K_\omega^T = 0.75K_{\omega,max}^T$

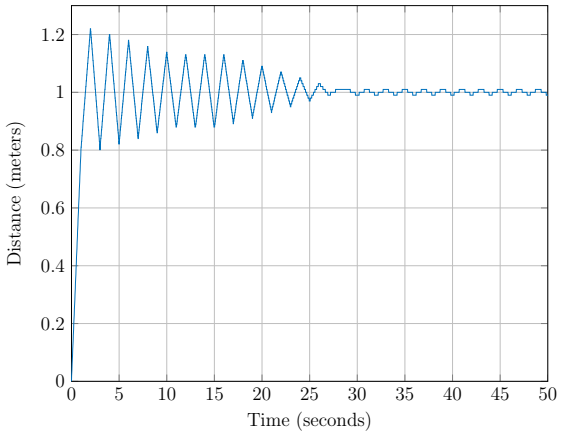

Figure 33: The orientation of the robot over time for $K_\omega^T = K_{\omega,max}^T$.

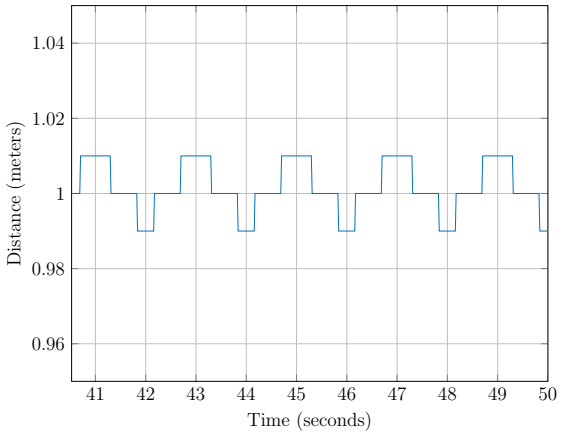

Figure 34: The steady state orientation of the robot for $K_\omega^T = K_{\omega,max}^T$

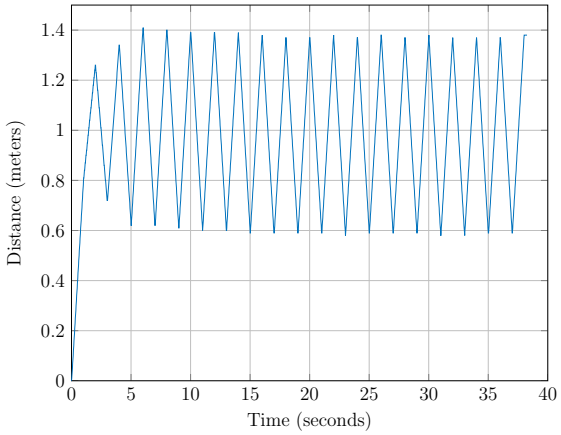

Figure 35: The orientation of the robot over time for $K_\omega^T = 1.1K_{\omega,max}^T$. The system is marginally stable

Task 14

$$d_p[k+1] = p(\theta[k+1] - \theta_g) \tag{8}$$

But

$$\theta[k+1] = \theta[k] + T_s \frac{R}{L} u_\Psi^T[k]$$

Hence equation 8 becomes

$$
\begin{aligned}
d_p[k+1] &= p(\theta[k] + T_s\frac{R}{L}u_\Psi^T[k] - \theta_g) \\
&= p(\theta[k] + T_s\frac{R}{L}K_\Psi^T d_p[k] - \theta_g) \\
&= pT_s\frac{R}{L}K_\Psi^T d_p[k] + p(\theta[k] - \theta_g) \\
&= pT_s\frac{R}{L}K_\Psi^T d_p[k] + d_p[k] \\
&= d_p[k](1 + pT_s\frac{R}{L}K_\Psi^T d_p[k])
\end{aligned}
$$

In order for this system to be stable, that is, $d_p \to 0$ as $k \to \infty$, the solution of the equation inside the parentheses should lie inside the unit circle:

$$
\begin{aligned}
\left|1+pT_s\frac{R}{L}K_\omega^T\right| &< 1 \\
-1 < 1+pT_s\frac{R}{L}K_\omega^T &< 1 \\
-2 < pT_s\frac{R}{L}K_\omega^T &< 0 \\
-\frac{2L}{pT_sR} < K_\omega^T &< 0
\end{aligned} \tag{9}
$$

Hence, the maximum value K_ω^T can take for the system to be marginally stable is $K_{\omega,max}^T = 0$.

Theoretically, the value of K_ω^T can be chosen to be any value inside the interval defined in inequality 6. However, first, it would be wise to choose a value that is far enough from the maximum value so as to avoid overshoot, but close enough to it, so that convergence happens in reasonable time. Hence, in practice, it is reasonable that one would need to experiment with different values and choose one that results in balancing a small angular error, a minimal overshoot, if any, and a quick enough settling time.

Task 15

Inequality 9 tells us that the higher the value of p, the broader the region of values for K_Ψ^T is so that the systems is stable. Hence, the lower the value of p is, the worse the robot's ability to follow a line is.

Task 16

This part of the controller is responsible for compensating for rotational errors during translation. Since the translational velocity u_ω is zero, it is expected that the robot will not rotate away from its original bearing. Figure 36 plots the robot's bearing with regard to its original bearing of 0 degrees over time for $K_\Psi^T = 0.5K_{\Psi,min}^T$.

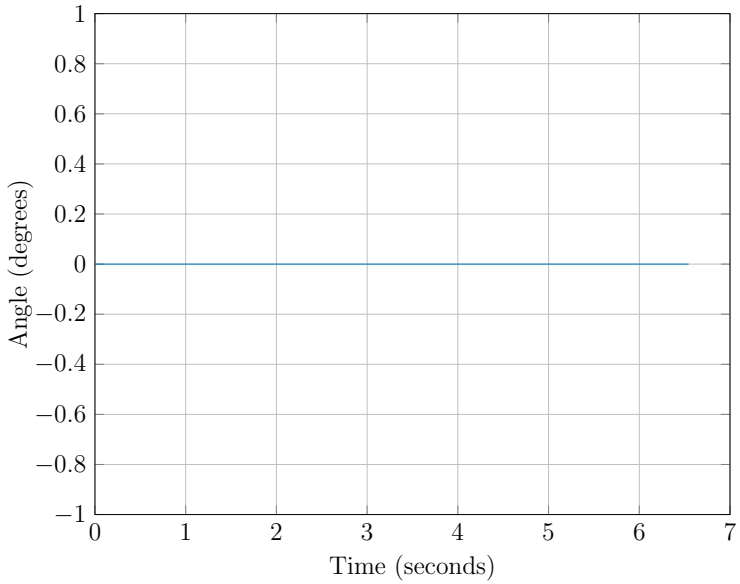

Figure 36: The angular displacement of the robot from its original bearing over time for $K_{\Psi}^{T} = 0.5K_{\Psi,min}^{T}$

Task 17

Figures 37, 39, 41, 43 and show the displacemental error of the robot for different values of K_{ω}^{T} inside the interval set by inequality 9. Figures 38, 40, 42 and 44 focus on the steady-state displacemental error. Figure 45 illustrates the $d_0[k]$ error, which is at all times zero.

The evolution of the bearing and displacement error is the same when both of the translational controllers are enabled compared to when only one of them is enabled. This happens because the behaviour of each controller does not affect the behaviour of the other, since this is an ideal system. In reality, we expect that the angular error will be non-zero.

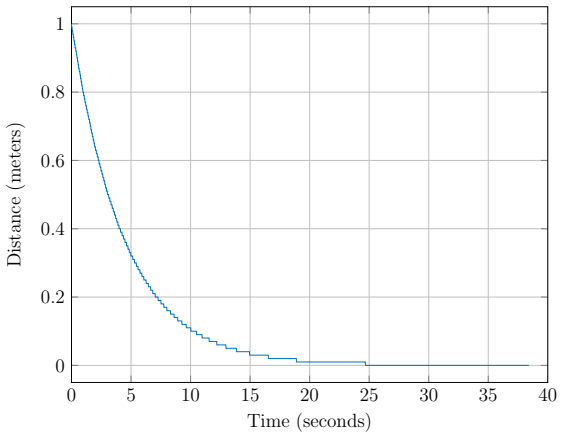

Figure 37: The error in displacement of the robot over time for $K_{\omega}^{T} = 0.1K_{\omega,max}^{T}$

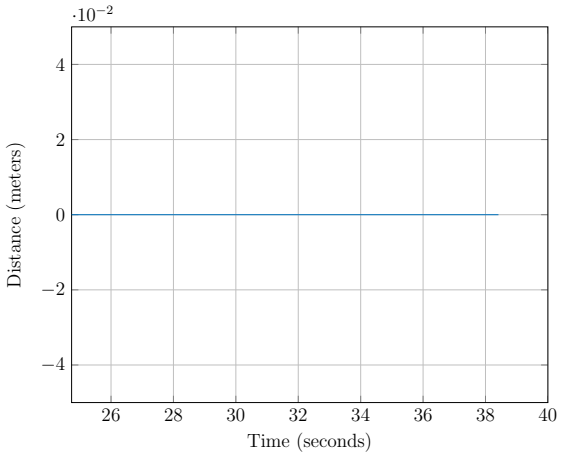

Figure 38: The steady state error in displacement of the robot for $K_{\omega}^{T} = 0.1K_{\omega,max}^{T}$

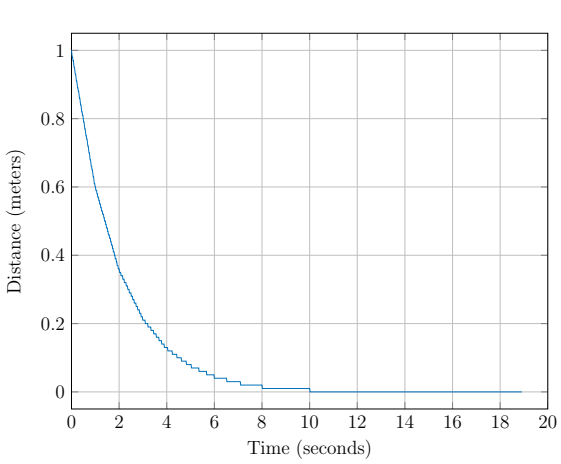

Figure 39: The error in displacement of the robot over time for $K_\omega^T = 0.2K_{\omega,max}^T$

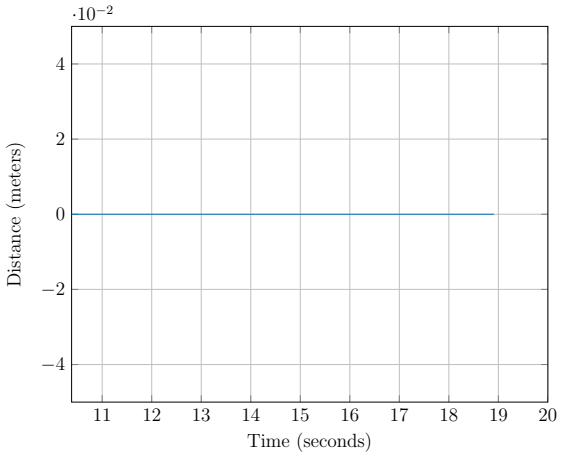

Figure 40: The steady state error in displacement of the robot for $K_\omega^T = 0.2K_{\omega,max}^T$

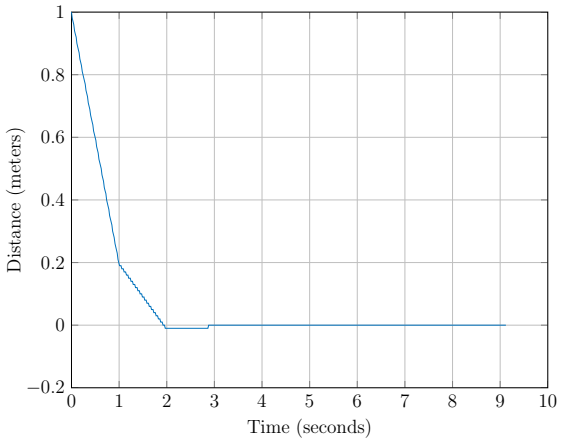

Figure 41: The error in displacement of the robot over time for $K_\omega^T = 0.5K_{\omega,max}^T$

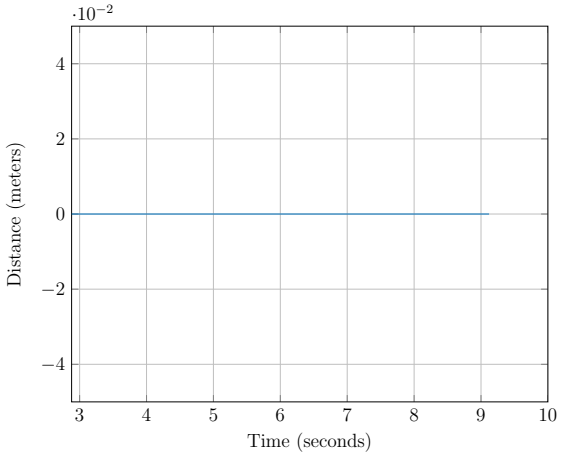

Figure 42: The steady state error in displacement of the robot for $K_\omega^T = 0.5K_{\omega,max}^T$

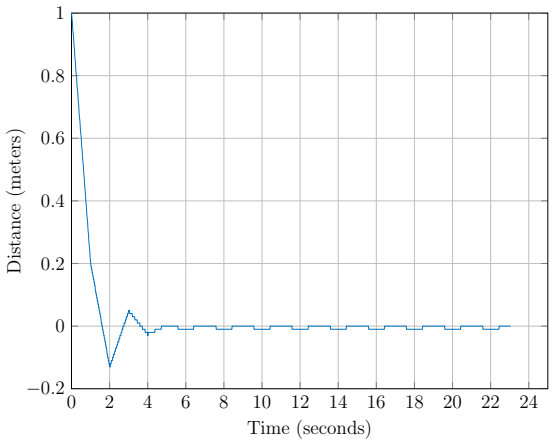

Figure 43: The error in displacement of the robot over time for $K_\omega^T = 0.75K_{\omega,max}^T$

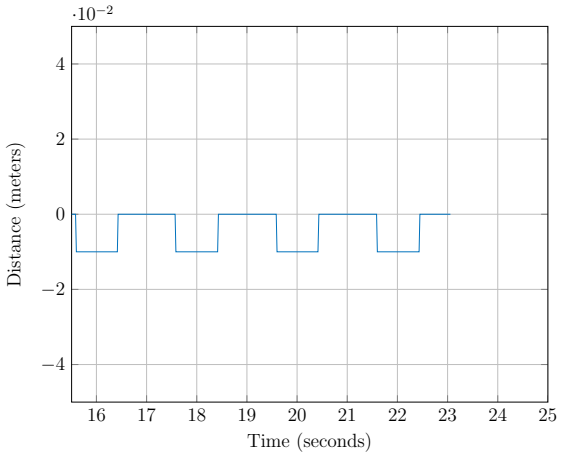

Figure 44: The steady state error in displacement of the robot for $K_\omega^T = 0.75K_{\omega,max}^T$

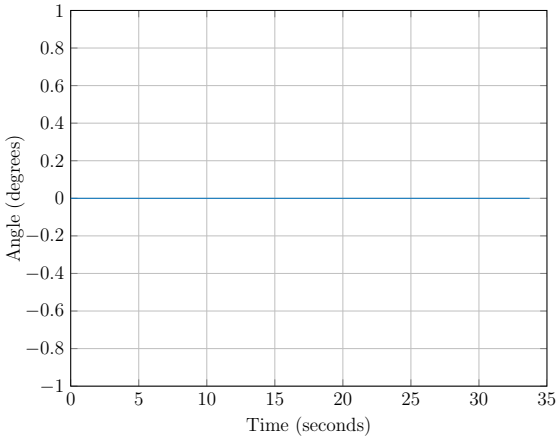

Figure 45: The steady state error in orientation of the robot for all legitimate values of K_ω^T

Task 18

Task 19

Evaluating the performance of the hybrid automaton primarily involves the evaluation of the steady-state errors regarding the position and angle of the robot with regard to the selected goal position. In order to obtain a broader understanging of how the four K_* gains influence the trajectory of the robot, twelve combinations were considered for the 4-tuple

$$(K_\Psi^R, K_\omega^T, K_\omega^R, K_\Psi^T)$$

where

$$K_\Psi^R \in \{0.1, 0.2, 0.5\} \cdot K_{\Psi,max}^R$$

$$K_\omega^T \in \{0.1, 0.2, 0.5, 0.75\} \cdot K_{\omega,max}^T$$

$$K_{\omega}^{R} = 0.5K_{\omega,max}^{R}, \text{ and } K_{\Psi}^{T} = -0.5K_{\Psi,min}^{T}$$

Notice the minus sign for K_{Ψ}^{T}. Although theoretically (and using the approximative form for $d_p[k]$) this gain should be negative, simulations showed that the robot achieved lower levels of both displacemental and angular errors when considered positive[1]. For purposes of homogeneity we shall denote $K_{\Psi,max}^{T} = -K_{\Psi,min}^{T}$, so $K_{\Psi}^{T} = 0.5K_{\Psi,max}^{T}$.

Figures 46 - 81 illustrate the evolution of the distance of the robot in relation to its goal, the angular error, and the discrete state trajectories, over time, for the aforementioned combinations of values of the gains K_*. The goal was set to be node 1 $N1(-0.37, 1.68)$, and the robot's initial pose was $(x_0, y_0, \theta_0) \equiv (0, 0, 0)$. Hence, the distance to the goal was $d_g = 1.7203$ meters and the angle to the goal $\theta^R = 102.42°$. The distance and angle tolerance thresholds where taken to be $d_{th} = 2$ cm and $\theta_{th} = 2°$ respectively.

Since the actual final pose is not defined deterministically, five simulations of each possible combination of settings for the aforementioned 4-tuple were conducted. Hence, all the following figures express the mean steady-state positional and angular errors across five runs.

Table 1 illustrates the steady-state errors e_d and e_θ regarding the distance and the angle that the robot had to travel, respectively.

$K_{\Psi}^{R}/K_{\Psi,max}^{R}$	$K_{\omega}^{T}/K_{\omega,max}^{T}$	e_d (cm)	e_θ (deg)
0.1	0.1	1.73	0.329
0.1	0.2	0.60	0.144
0.1	0.5	0.90	0.330
0.1	0.75	1.9	0.054
0.2	0.1	1.47	0.419
0.2	0.2	1.21	0.308
0.2	0.5	0.67	0.116
0.2	0.75	2.12	0.026
0.5	0.1	1.26	0.303
0.5	0.2	0.75	0.585
0.5	0.5	1.05	0.695
0.5	0.75	0.86	0.347

Table 1: Mean steady-state errors regarding the distance and bearing to Node 1 for the 12 different combinations considered for the 4-tuple $(K_{\Psi}^{R}, K_{\omega}^{T}, K_{\omega}^{R}, K_{\Psi}^{T})$

The combination of the two control components made it possible for the robot to move to any location inside the simulation environment. In particular, for the single goal considered here, the controller made it possible for the robot to approach node 1 within a radius of length d_{th} (with one exception, when $(K_{\Psi}^{R}/K_{\Psi,max}^{R}, K_{\omega}^{T}/K_{\omega,max}^{T}) \equiv (0.2, 0.75)$) and with a bearing well within the 2° upper threshold. The second component of the line-following controller was partly responsible for reducing the bearing errors compared to the case when only the rotational controller was enabled. However, in order for the second component's input to be able to kick in in the first place, it was necessary to limit the translational velocity of the robot to a value of $u_\omega = 400$, so as to permit the correctional input of this component to become active, since there is an upper limit to the velocities the robot can achieve, either in simulation or in real-life.

[1] Analysis on Task 14 showed that $K_{\Psi,min}^{T}$ is considered negative

The discrete state trajectory figures express what was expected: as the value of a gain K_* increases, the time that the robot stays in the corresponding state decreases. What was not expected, though, was the temporary spikes into state `Stop` for all cases when $K_\omega^T / K_{\omega,max}^T = 0.75$. This makes sence, since that high a value for the gain of the translational part of the line-following controller makes the robot overshoot the goal. Its momentum is such that while it approaches the goal within d_{th} m and its state transitions from `Translation` to `Stop`, it cannot physically stop and steps out of the circle with radius d_{th}, and thus its state goes back to `Translation`. The duration the robot stays at state `Stop` is the duration of time it spends inside this virual circle with radius d_{th}. This time interval is observed to be unequal among all three cases, due to the fact that the robot travels forwards (part I of the line-following controller) and rotates (part II of the line-following controller) simultaneously.

The following sections illustrate the displacemental and angular errors and the discrete state trajectory over time for different values of the four gains.

$$\left(\frac{K_\Psi^R}{K_{\Psi,max}^R}, \frac{K_\omega^T}{K_{\omega,max}^T}, \frac{K_\omega^R}{K_{\omega,max}^R}, \frac{K_\Psi^T}{K_{\Psi,max}^T} \right) \equiv (0.1, 0.1, 0.5, 0.5)$$

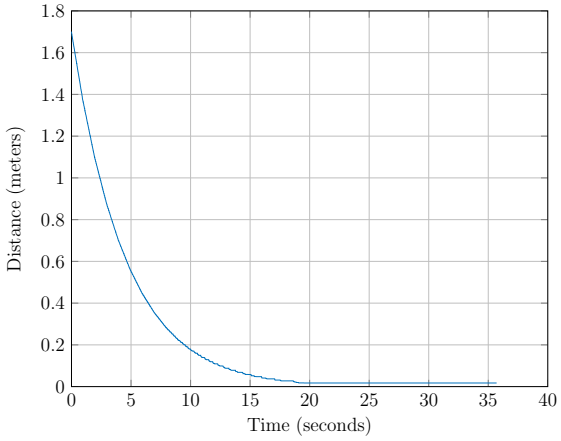

Figure 46: The error in displacement of the robot over time for $(K_\Psi^R, K_\omega^T) \equiv (0.1K_{\Psi,max}^R, 0.1K_{\omega,max}^T)$

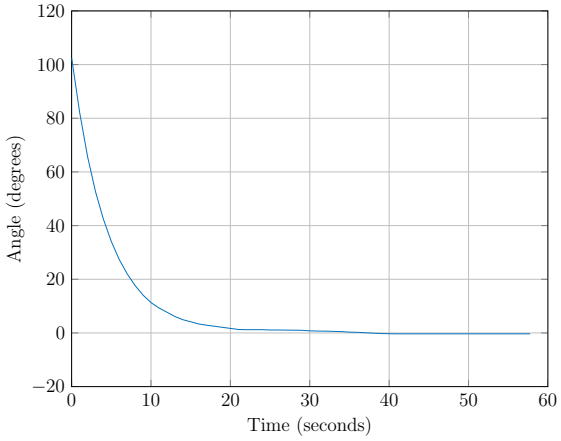

Figure 47: The error in bearing of the robot over time for $(K_\Psi^R, K_\omega^T) \equiv (0.1K_{\Psi,max}^R, 0.1K_{\omega,max}^T)$

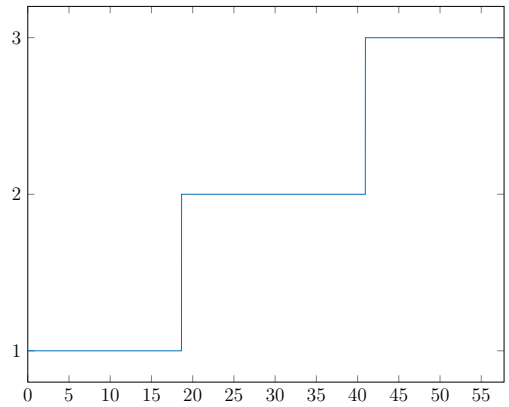

Figure 48: The discrete state trajectory for $(K_{\Psi}^{R}, K_{\omega}^{T}) \equiv (0.1K_{\Psi,max}^{R}, 0.1K_{\omega,max}^{T})$. 1 denotes `Rotation`, 2 denotes `Translation` and 3 denotes `Stop`

$$\left(\frac{K_{\Psi}^{R}}{K_{\Psi,max}^{R}}, \frac{K_{\omega}^{T}}{K_{\omega,max}^{T}}, \frac{K_{\omega}^{R}}{K_{\omega,max}^{R}}, \frac{K_{\Psi}^{T}}{K_{\Psi,max}^{T}}\right) \equiv (0.1, 0.2, 0.5, 0.5)$$

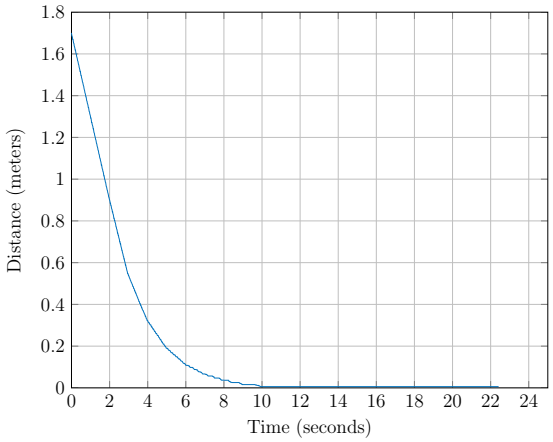

Figure 49: The error in displacement of the robot over time for $(K_{\Psi}^{R}, K_{\omega}^{T}) \equiv (0.1K_{\Psi,max}^{R}, 0.2K_{\omega,max}^{T})$

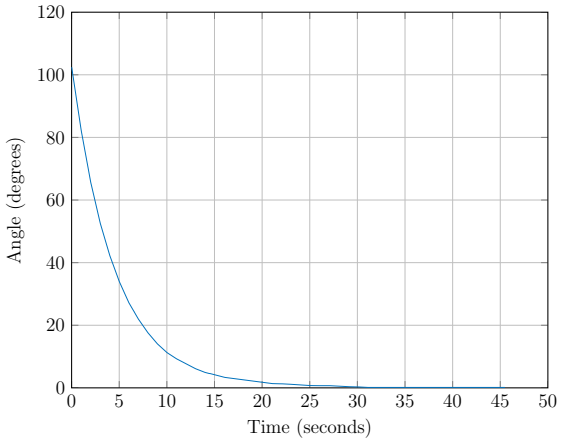

Figure 50: The error in bearing of the robot over time for $(K_{\Psi}^{R}, K_{\omega}^{T}) \equiv (0.1K_{\Psi,max}^{R}, 0.2K_{\omega,max}^{T})$

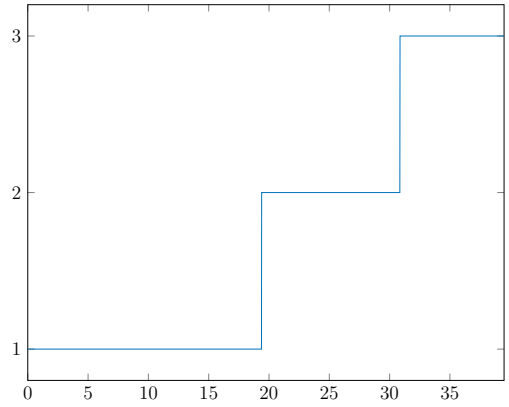

Figure 51: The discrete state trajectory for $(K_{\Psi}^{R}, K_{\omega}^{T}) \equiv (0.1K_{\Psi,max}^{R}, 0.2K_{\omega,max}^{T})$. 1 denotes `Rotation`, 2 denotes `Translation` and 3 denotes `Stop`

$$\left(\frac{K_{\Psi}^{R}}{K_{\Psi,max}^{R}}, \frac{K_{\omega}^{T}}{K_{\omega,max}^{T}}, \frac{K_{\omega}^{R}}{K_{\omega,max}^{R}}, \frac{K_{\Psi}^{T}}{K_{\Psi,max}^{T}}\right) \equiv (0.1, 0.5, 0.5, 0.5)$$

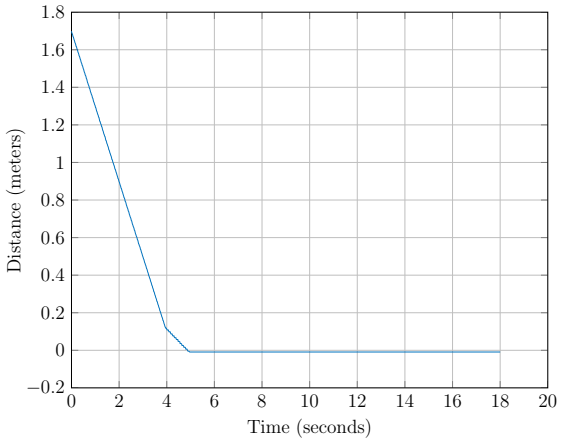

Figure 52: The error in displacement of the robot over time for $(K_{\Psi}^{R}, K_{\omega}^{T}) \equiv (0.1K_{\Psi,max}^{R}, 0.5K_{\omega,max}^{T})$

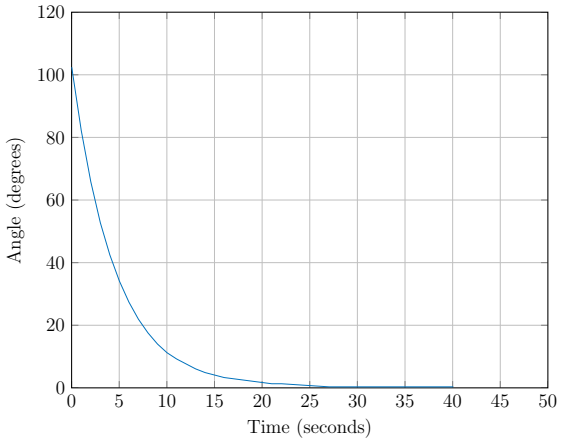

Figure 53: The error in bearing of the robot over time for $(K_{\Psi}^{R}, K_{\omega}^{T}) \equiv (0.1K_{\Psi,max}^{R}, 0.5K_{\omega,max}^{T})$

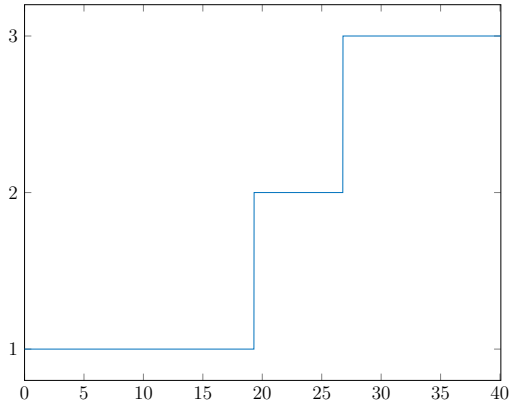

Figure 54: The discrete state trajectory for $(K_{\Psi}^{R}, K_{\omega}^{T}) \equiv (0.1K_{\Psi,max}^{R}, 0.5K_{\omega,max}^{T})$. 1 denotes `Rotation`, 2 denotes `Translation` and 3 denotes `Stop`

$$\left(\frac{K_{\Psi}^{R}}{K_{\Psi,max}^{R}}, \frac{K_{\omega}^{T}}{K_{\omega,max}^{T}}, \frac{K_{\omega}^{R}}{K_{\omega,max}^{R}}, \frac{K_{\Psi}^{T}}{K_{\Psi,max}^{T}}\right) \equiv (0.1, 0.75, 0.5, 0.5)$$

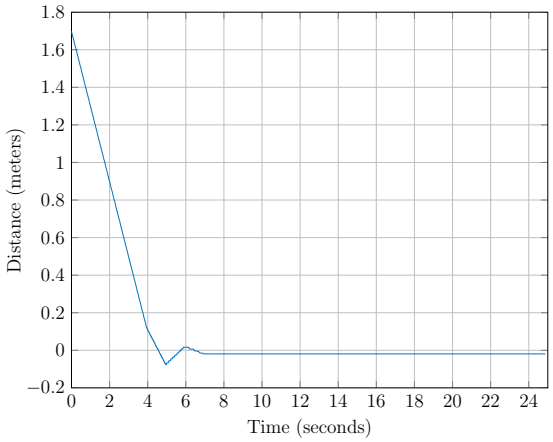

Figure 55: The error in displacement of the robot over time for $(K_{\Psi}^{R}, K_{\omega}^{T}) \equiv (0.1K_{\Psi,max}^{R}, 0.75K_{\omega,max}^{T})$

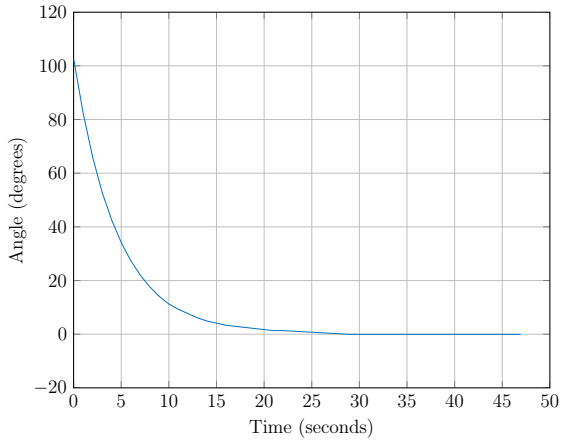

Figure 56: The error in bearing of the robot over time for $(K_{\Psi}^{R}, K_{\omega}^{T}) \equiv (0.1K_{\Psi,max}^{R}, 0.75K_{\omega,max}^{T})$

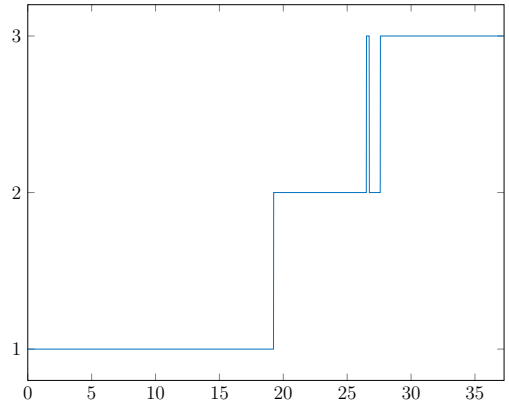

Figure 57: The discrete state trajectory for $(K_{\Psi}^{R}, K_{\omega}^{T}) \equiv (0.1K_{\Psi,max}^{R}, 0.75K_{\omega,max}^{T})$. 1 denotes `Rotation`, 2 denotes `Translation` and 3 denotes `Stop`

$$\left(\frac{K_{\Psi}^{R}}{K_{\Psi,max}^{R}}, \frac{K_{\omega}^{T}}{K_{\omega,max}^{T}}, \frac{K_{\omega}^{R}}{K_{\omega,max}^{R}}, \frac{K_{\Psi}^{T}}{K_{\Psi,max}^{T}}\right) \equiv (0.2, 0.1, 0.5, 0.5)$$

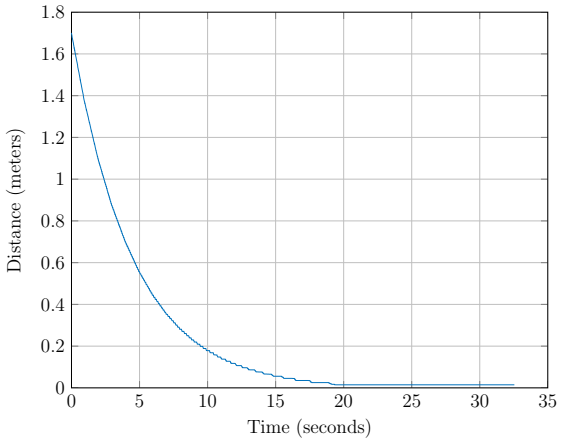

Figure 58: The error in displacement of the robot over time for $(K_{\Psi}^{R}, K_{\omega}^{T}) \equiv (0.2K_{\Psi,max}^{R}, 0.1K_{\omega,max}^{T})$

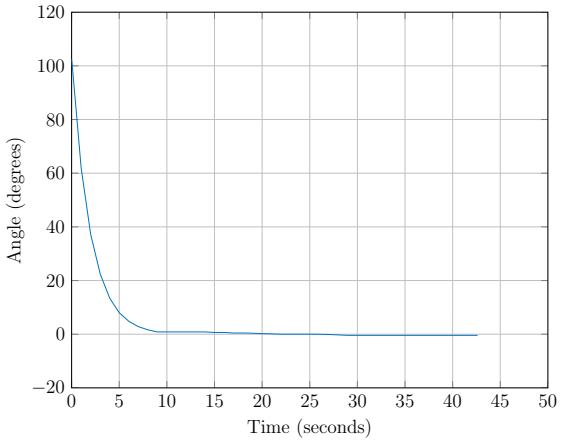

Figure 59: The error in bearing of the robot over time for $(K_{\Psi}^{R}, K_{\omega}^{T}) \equiv (0.2K_{\Psi,max}^{R}, 0.1K_{\omega,max}^{T})$

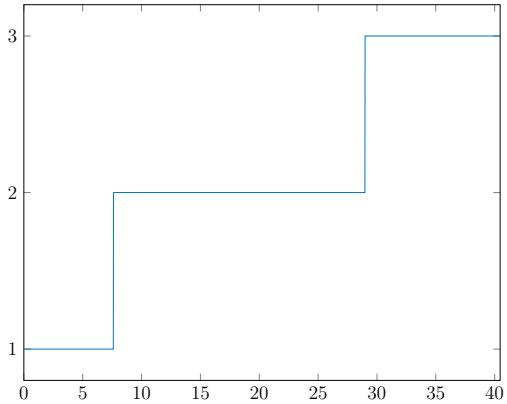

Figure 60: The discrete state trajectory for $(K_{\Psi}^{R}, K_{\omega}^{T}) \equiv (0.1K_{\Psi,max}^{R}, 0.1K_{\omega,max}^{T})$. 1 denotes `Rotation`, 2 denotes `Translation` and 3 denotes `Stop`

$$\left(\frac{K_{\Psi}^{R}}{K_{\Psi,max}^{R}}, \frac{K_{\omega}^{T}}{K_{\omega,max}^{T}}, \frac{K_{\omega}^{R}}{K_{\omega,max}^{R}}, \frac{K_{\Psi}^{T}}{K_{\Psi,max}^{T}}\right) \equiv (0.2, 0.2, 0.5, 0.5)$$

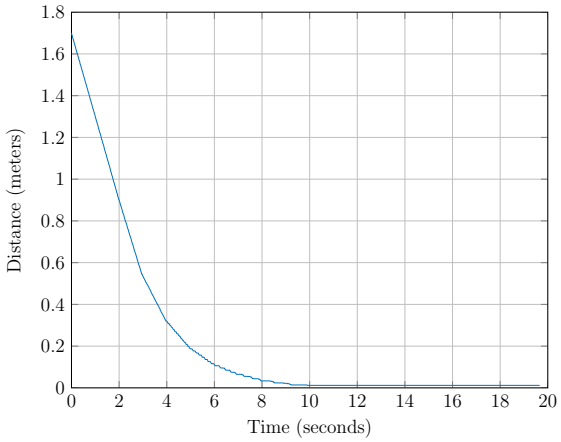

Figure 61: The error in displacement of the robot over time for $(K_{\Psi}^{R}, K_{\omega}^{T}) \equiv (0.2K_{\Psi,max}^{R}, 0.2K_{\omega,max}^{T})$

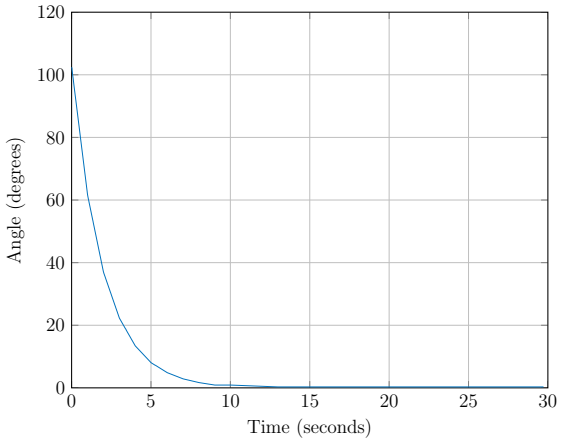

Figure 62: The error in bearing of the robot over time for $(K_{\Psi}^{R}, K_{\omega}^{T}) \equiv (0.2K_{\Psi,max}^{R}, 0.2K_{\omega,max}^{T})$

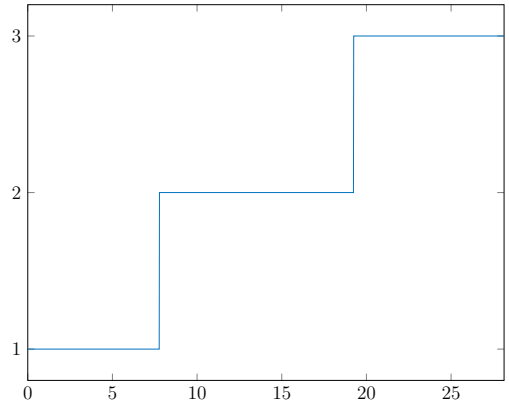

Figure 63: The discrete state trajectory for $(K_{\Psi}^{R}, K_{\omega}^{T}) \equiv (0.2K_{\Psi,max}^{R}, 0.2K_{\omega,max}^{T})$. 1 denotes `Rotation`, 2 denotes `Translation` and 3 denotes `Stop`

$$\left(\frac{K_{\Psi}^{R}}{K_{\Psi,max}^{R}}, \frac{K_{\omega}^{T}}{K_{\omega,max}^{T}}, \frac{K_{\omega}^{R}}{K_{\omega,max}^{R}}, \frac{K_{\Psi}^{T}}{K_{\Psi,max}^{T}}\right) \equiv (0.2, 0.5, 0.5, 0.5)$$

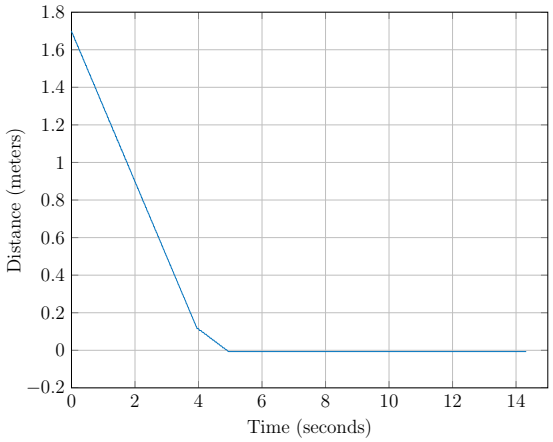

Figure 64: The error in displacement of the robot over time for $(K_{\Psi}^{R}, K_{\omega}^{T}) \equiv (0.2K_{\Psi,max}^{R}, 0.5K_{\omega,max}^{T})$

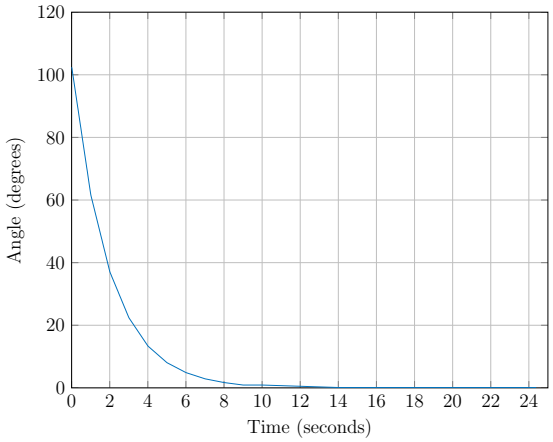

Figure 65: The error in bearing of the robot over time for $(K_{\Psi}^{R}, K_{\omega}^{T}) \equiv (0.2K_{\Psi,max}^{R}, 0.5K_{\omega,max}^{T})$

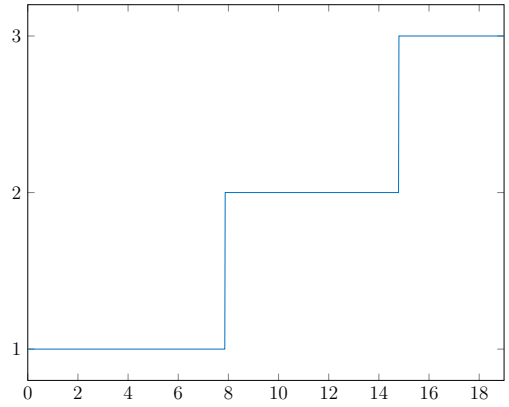

Figure 66: The discrete state trajectory for $(K_{\Psi}^{R}, K_{\omega}^{T}) \equiv (0.2K_{\Psi,max}^{R}, 0.5K_{\omega,max}^{T})$. 1 denotes `Rotation`, 2 denotes `Translation` and 3 denotes `Stop`

$$\left(\frac{K_{\Psi}^{R}}{K_{\Psi,max}^{R}}, \frac{K_{\omega}^{T}}{K_{\omega,max}^{T}}, \frac{K_{\omega}^{R}}{K_{\omega,max}^{R}}, \frac{K_{\Psi}^{T}}{K_{\Psi,max}^{T}}\right) \equiv (0.2, 0.75, 0.5, 0.5)$$

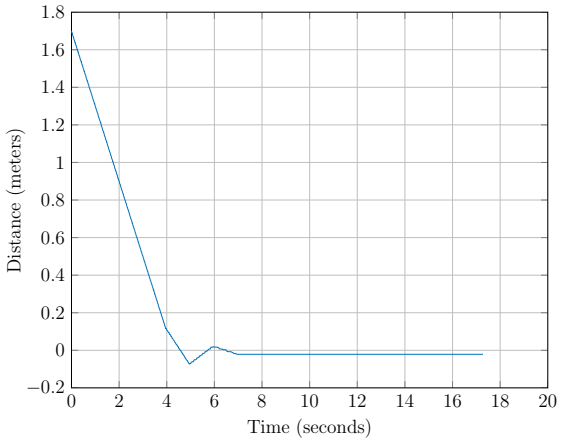

Figure 67: The error in displacement of the robot over time for $(K_{\Psi}^{R}, K_{\omega}^{T}) \equiv (0.2K_{\Psi,max}^{R}, 0.75K_{\omega,max}^{T})$

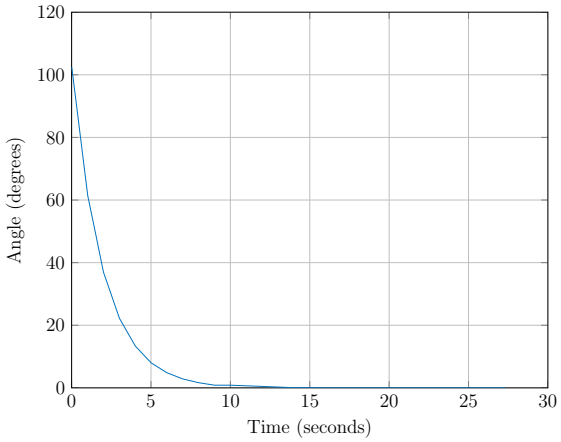

Figure 68: The error in bearing of the robot over time for $(K_{\Psi}^{R}, K_{\omega}^{T}) \equiv (0.2K_{\Psi,max}^{R}, 0.75K_{\omega,max}^{T})$

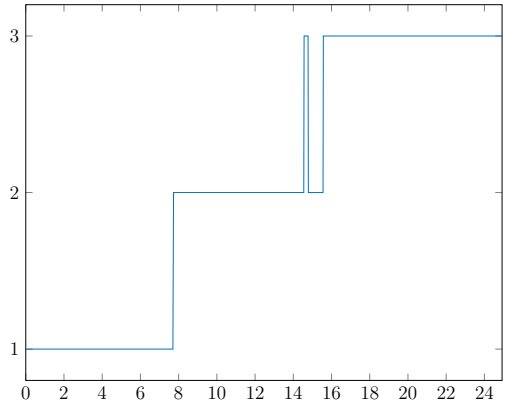

Figure 69: The discrete state trajectory for $(K_{\Psi}^{R}, K_{\omega}^{T}) \equiv (0.2K_{\Psi,max}^{R}, 0.75K_{\omega,max}^{T})$. 1 denotes `Rotation`, 2 denotes `Translation` and 3 denotes `Stop`

$$\left(\frac{K_{\Psi}^{R}}{K_{\Psi,max}^{R}}, \frac{K_{\omega}^{T}}{K_{\omega,max}^{T}}, \frac{K_{\omega}^{R}}{K_{\omega,max}^{R}}, \frac{K_{\Psi}^{T}}{K_{\Psi,max}^{T}}\right) \equiv (0.5, 0.1, 0.5, 0.5)$$

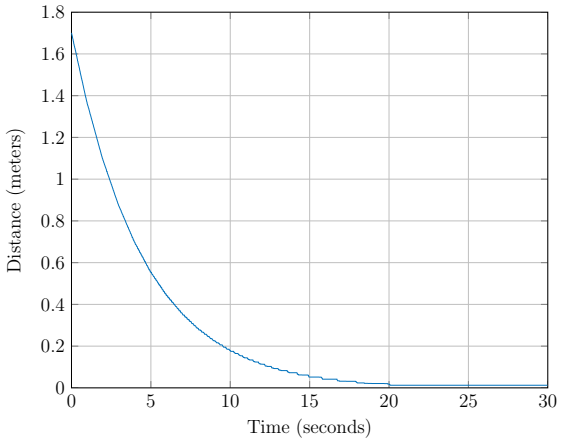

Figure 70: The error in displacement of the robot over time for $(K_{\Psi}^{R}, K_{\omega}^{T}) \equiv (0.5K_{\Psi,max}^{R}, 0.1K_{\omega,max}^{T})$

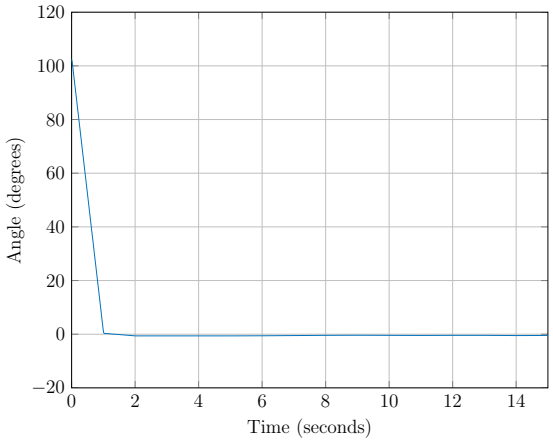

Figure 71: The error in bearing of the robot over time for $(K_{\Psi}^{R}, K_{\omega}^{T}) \equiv (0.5K_{\Psi,max}^{R}, 0.1K_{\omega,max}^{T})$

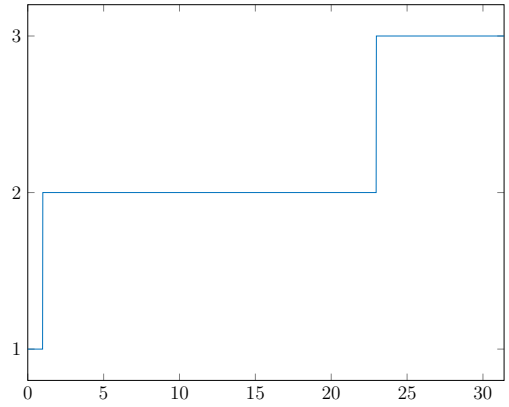

Figure 72: The discrete state trajectory for $(K_{\Psi}^{R}, K_{\omega}^{T}) \equiv (0.5K_{\Psi,max}^{R}, 0.1K_{\omega,max}^{T})$. 1 denotes `Rotation`, 2 denotes `Translation` and 3 denotes `Stop`

$$\left(\frac{K_{\Psi}^{R}}{K_{\Psi,max}^{R}}, \frac{K_{\omega}^{T}}{K_{\omega,max}^{T}}, \frac{K_{\omega}^{R}}{K_{\omega,max}^{R}}, \frac{K_{\Psi}^{T}}{K_{\Psi,max}^{T}}\right) \equiv (0.5, 0.2, 0.5, 0.5)$$

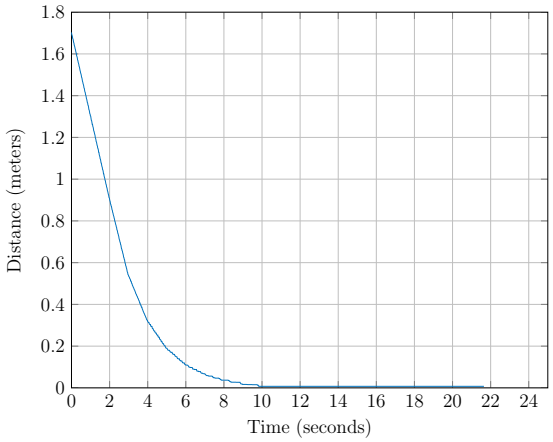

Figure 73: The error in displacement of the robot over time for $(K_{\Psi}^{R}, K_{\omega}^{T}) \equiv (0.5K_{\Psi,max}^{R}, 0.2K_{\omega,max}^{T})$

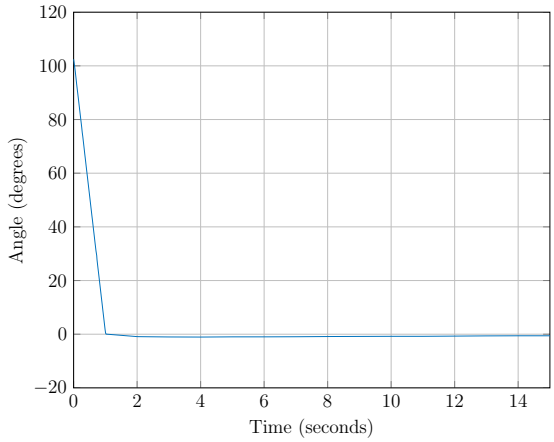

Figure 74: The error in bearing of the robot over time for $(K_{\Psi}^{R}, K_{\omega}^{T}) \equiv (0.5K_{\Psi,max}^{R}, 0.2K_{\omega,max}^{T})$

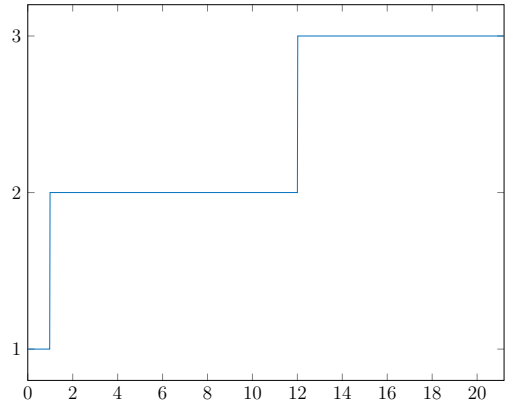

Figure 75: The discrete state trajectory for $(K_{\Psi}^{R}, K_{\omega}^{T}) \equiv (0.5K_{\Psi,max}^{R}, 0.2K_{\omega,max}^{T})$. 1 denotes `Rotation`, 2 denotes `Translation` and 3 denotes `Stop`

$$\left(\frac{K_{\Psi}^{R}}{K_{\Psi,max}^{R}}, \frac{K_{\omega}^{T}}{K_{\omega,max}^{T}}, \frac{K_{\omega}^{R}}{K_{\omega,max}^{R}}, \frac{K_{\Psi}^{T}}{K_{\Psi,max}^{T}}\right) \equiv (0.5, 0.5, 0.5, 0.5)$$

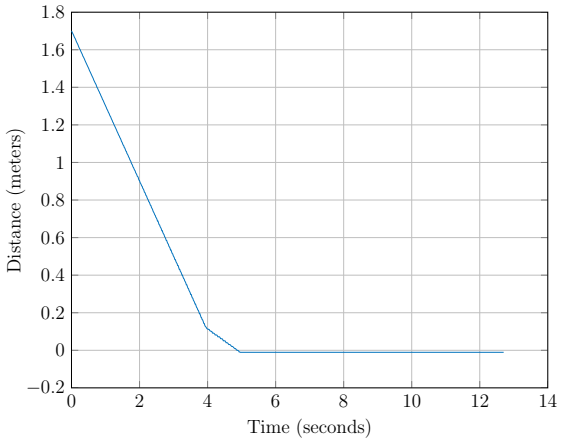

Figure 76: The error in displacement of the robot over time for $(K_{\Psi}^{R}, K_{\omega}^{T}) \equiv (0.5K_{\Psi,max}^{R}, 0.5K_{\omega,max}^{T})$

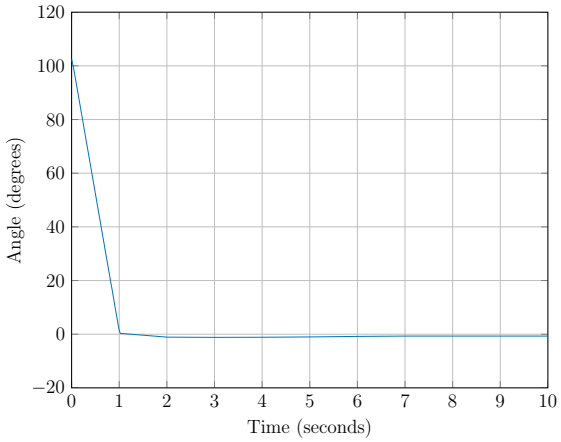

Figure 77: The error in bearing of the robot over time for $(K_{\Psi}^{R}, K_{\omega}^{T}) \equiv (0.5K_{\Psi,max}^{R}, 0.5K_{\omega,max}^{T})$

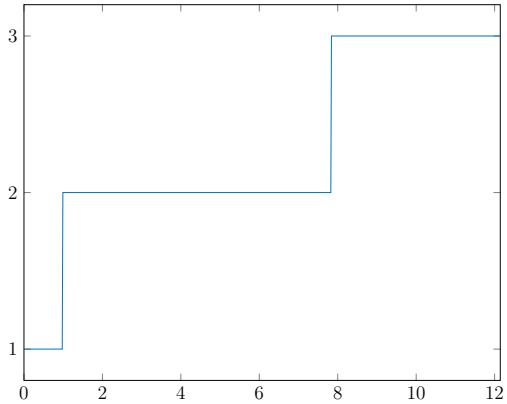

Figure 78: The discrete state trajectory for $(K_{\Psi}^{R}, K_{\omega}^{T}) \equiv (0.5K_{\Psi,max}^{R}, 0.5K_{\omega,max}^{T})$. 1 denotes `Rotation`, 2 denotes `Translation` and 3 denotes `Stop`

$$\left(\frac{K_{\Psi}^{R}}{K_{\Psi,max}^{R}}, \frac{K_{\omega}^{T}}{K_{\omega,max}^{T}}, \frac{K_{\omega}^{R}}{K_{\omega,max}^{R}}, \frac{K_{\Psi}^{T}}{K_{\Psi,max}^{T}}\right) \equiv (0.5, 0.75, 0.5, 0.5)$$

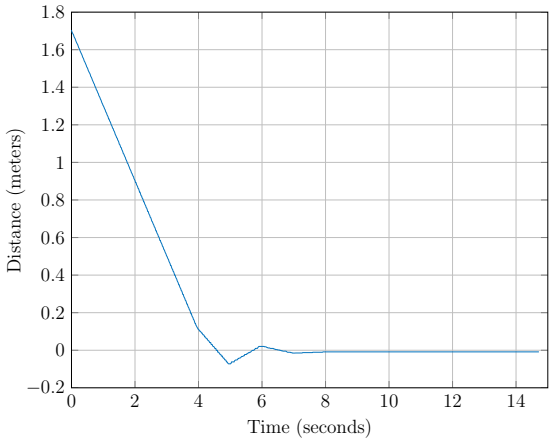

Figure 79: The error in displacement of the robot over time for $(K_{\Psi}^{R}, K_{\omega}^{T}) \equiv (0.5K_{\Psi,max}^{R}, 0.75K_{\omega,max}^{T})$

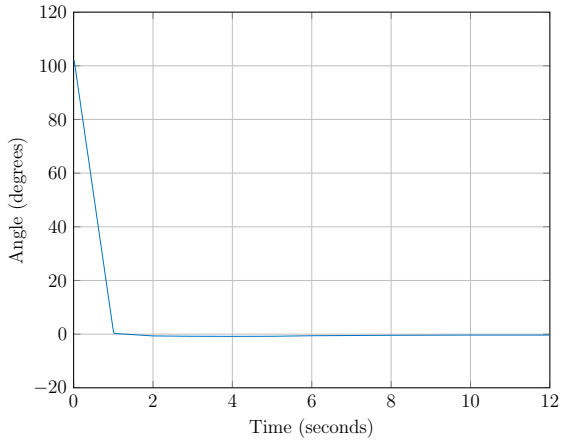

Figure 80: The error in bearing of the robot over time for $(K_{\Psi}^{R}, K_{\omega}^{T}) \equiv (0.5K_{\Psi,max}^{R}, 0.75K_{\omega,max}^{T})$

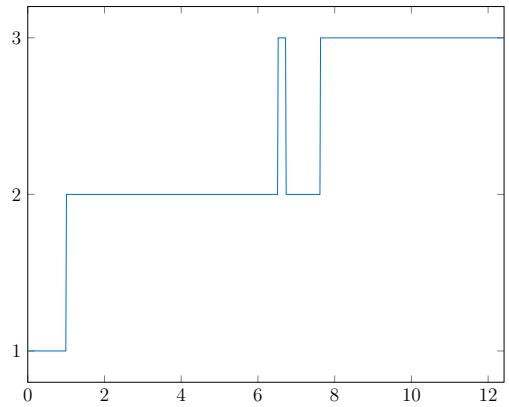

Figure 81: The discrete state trajectory for $(K_{\Psi}^{R}, K_{\omega}^{T}) \equiv (0.5K_{\Psi,max}^{R}, 0.75K_{\omega,max}^{T})$. 1 denotes `Rotation`, 2 denotes `Translation` and 3 denotes `Stop`

Task 20

Task 21

Task 22